Journal of Palaeosciences 71(2022): 75–88
0031–0174/2022

Palaeoclimatic variability during last eight millennia from a morainal lake in Zanskar, northwest Himalaya, India

BINITA PHARTIYAL[1*], SHEIKH NAWAZ ALI[1], ANUPAM SHARMA[1], SHAILESH AGRAWAL[1], DEBARATI NAG[1], POOJA TIWARI[1], MOHAN KUMAR[1], P. MORTHEKAI[1], PAWAN GOVIL[1], BISWAJEET THAKUR[1], RAVI BHUSHAN[2], PARTHA SARATHI JENA[2] AND A. SHIVAM[2]

[1]*Birbal Sahni Institute of Palaeosciences, 53 University Road, Lucknow 226 007, India.*
[2]*Physical Research Laboratory, University Area, Ahmadabad 380009, India.*
[*]*Corresponding author: binita_phartiyal@bsip.res.in; binitaphartiyal@gmail.com*

(Received 29 April, 2022; revised version accepted 20 June, 2022)

ABSTRACT

Phartiyal B, Ali SN, Sharma A, Agrawal S, Nag D, Tiwari P, Kumar M, Morthekai P, Govil P, Thakur B, Bhushan R, Jena PS & Shivam A 2022. Palaeoclimatic variability during last eight millennia from a morainal lake in Zanskar, northwest Himalaya, India. Journal of Palaeosciences 71(1): 75–88.

Centennial–scale palaeoenvironmental variability has been deduced during past eight millennia using multi–proxy study (textural analysis, environmental magnetic parameters, stable carbon isotopes, palynofacies and elemental concentration), from Khangok–Padam in Zanskar Valley, northwest Himalaya. The multi–proxy record from this morainal lake spanning last ~8200 cal years BP has revealed four hydroclimatic phases. The overall progressively improving hydroclimatic trend is indicated by multi proxy study: sediment size/texture (as a proxy for the energy condition and depositional environment), mineral magnetism (proxy for sediment flux or lithogenic input and lithologic variation), carbon isotope signature ($\delta^{13}C_{org}$) preserved in organic constituents of sediments (a proxy for palaeovegetation and climate change), elemental geochemistry (proxy for weathering and erosion) and selected samples for palynofacies data (a proxy for changes in biological organic matter). This improving hydroclimatic trend is however punctuated by an abrupt wet spell at ~6200–5200 cal years BP and relatively drier climate during the Little Ice Age between 1400 and 1900 CE. The main driving force implicated for the changes are seen to be the solar output variations. The area lying in a transitional climatic zone of NW Himalaya shows no emphatic record of the events like the 4200 cal. years BP, 2600 cal. years BP and Holocene Climatic Optima. Contrary to the earlier studies in the region (e.g. Tsokar and TsoMorari), our results show an improving hydroclimatic condition in this transition climatic zone between the Indian Summer Monsoon dominated Higher and westerly dominated Trans Himalaya.

Key–words—Holocene, Zanskar, Palaeoclimate, Hydroclimatic variability, Lakes, Moraines.

INTRODUCTION

THE Zanskar Valley in north–west Himalaya, is a climatologically transition zone between the two major climate circulation systems, viz. the south–west summer monsoon (ISM) and the winter Westerlies. This zone lying between the drier northern parts (Karakoram & Tibet) and the sub–humid areas towards south (Central Himalaya) is suggested to be suitable to understand the hydroclimatic fluctuations influenced by both the forcing namely the North Atlantic forcing (mid–latitude Westerlies) from the north and the ISM from the south (Ali *et al*., 2018, 2020). The present moisture/precipitation relief in the area is also due to the interaction of these weather systems; however, controversy over the past interaction/interplay of these weather systems persists, i.e. how these weather systems evolved and affected the hydroclimate of the region during the late Quaternary is uncertain (Prasad *et al*., 2014; Mishra *et al*., 2015).

As the Tibetan Plateau and Himalayan region are the most glaciated areas outside the Polar region, the glaciers and associated lakes are important and interrelated ecological components in these regions. Snow and glacier melt are

significant contributors to hydrologic systems, which are projected to be severely altered by temperature and precipitation changes. Furthermore, there are intimate linkages between lake level variations, climate changes, and glacier retreat that have an impact on the socio–economics of this high altitude and vulnerable region (Bolch *et al*., 2012; Sun *et al*., 2018). The late Holocene climate has relatively been stable, but within it, the low amplitude changes and abrupt short–lived climatic events like 4.2 ka event have resulted in drastic effects on the human civilizations, viz. Indus Valley (Harappan) Civilization and the Vedic Civilization, etc. (Sarkar *et al*., 2015; Kathayat *et al*., 2017). However, the amplitude of such climatic variations during the Holocene is relatively small because the boundary condition of climate system did not change much (Petit *et al*., 1999). Previous research from the Indian subcontinent revealed a strengthening of the monsoon during the early Holocene Period, but the pattern of mid–to late Holocene monsoon variability is still unclear and often suffers from age uncertainties (Prasad *et al*., 2014; Mishra *et al*., 2015; Sharma & Phartiyal, 2018; Banerji *et al*., 2020; Phartiyal *et al*., 2021a).

Investigations on the hydroclimatic variations in the NW Himalaya (influenced by monsoonal rains and westerly snow precipitation) are scarce and the limited number of studies carried out till now are generally restricted to the far north or northeast, where the influence of ISM is scanty. According to previous research, the paucity of signatures of low amplitude climatic shifts in the north–western Himalayan sedimentary archives is attributed to the buffering influence of snow runoff and reduced late Holocene ISM (Mishra *et al*., 2015). Palaeoclimatic studies from the north–western Himalaya so far have suggested a progressive decline in hydroclimatic conditions during the late Quaternary (Leipi *et al*., 2014; Mishra *et al*., 2015). We argue that in order to understand the hydroclimatic variations in the NW Himalayan sector during the mid–late Holocene, it is important to consider other areas that are located in the climatologically sensitive areas where both ISM and mid–latitude Westerlies are operating (transitional zones).

The morainal lakes, which are directly replenished by snow and glacial meltwater, give a rather full record of past climate variability due to continuous sedimentation. This continuous sedimentation is regulated by the meltwater and makes these lakes an exceptionally important palaeoclimatic archive providing short–term variability. Glaciers are believed to be among the most sensitive terrestrial recorders of climatic changes because they respond to the combined influence of precipitation (snowfall) and temperature (Pratt–Sitaula *et al*., 2011), and these changes are well recorded in the glacial lake sediments. In a range of spatial scales, different proxies, reflect varying impact of environmental factors and display varying strengths, limitations, and responses, therefore multi–proxy studies are desirable, as they will better reflect local to regional climatic conditions (Kathayat *et al*., 2017; Srivastava *et al*., 2018; Ali *et al*., 2020; Phartiyal *et al*., 2020). Palaeoenvironmental and palaeoclimatic reconstructions on lake sediments and the organic matter contained in it have generally been used in the Himalayan region, especially for alpine lake where organic matter could well represent the environment and climate fluctuations (Rawat *et al*., 2015; Phartiyal *et al*., 2020; 2021a). Hence with the above facts in view, we sampled a relict morainal lake deposit at Khangok, located south–east of the Padam Village, Zanskar Valley (transitional zone between ISM and Westerlies), with an objective to understand the spatial structure of mid–late Holocene climate changes and try to reveal the factors that are responsible for the sub–millennial scale climate variability. We aimed at multi–proxy data to reflect a clear picture of the local climatic conditions that is subsequently used for regional correlations as well. We intended for multi–proxy data to provide a holistic picture of local climatic conditions, which can then be utilised for regional correlations.

STUDY AREA

The current investigation was conducted on the sediment profile of a relict morainal lake (~33° 27' 05.88" N; 76° 52' 41.18" E; ~3700 m asl) at Khangok, in Padam Village, the sub–divisional capital of the Zanskar region, located ~200 km SE of the Kargil District, Ladakh, India (Fig. 1). The Zanskar Valley covers an area of ~7000 km^2 with an altitudinal range of ~3500 to 7000 m asl. It is drained by the Zanskar River, which moves through the mountain range from its origin at the DrangDrung Glacier adjacent to Pensi La (Dézes, 1999; Ali *et al*., 2018; Sharma & Shukla 2018) and joins the Indus River near Nimo Village. The sampling site falls on the northern flank of Higher Himalayan range and lies under a rain shadow zone of the ISM. Semi–arid desertic condition with very sparse steppe type vegetation restricted to moist patches only.

Geological and Geomorphological setting

Geologically lying in the Tethyan Himalayan region the Zanskar Valley comprises of the rocks of Higher Himalayan Crystalline Sequence (HHCS) and the sedimentary rocks (Proterozoic to Eocene) of Zanskar Range (Searle & Fryer, 1986). The HHCS are dominated by migmatitic ortho/para–gneisses and are broadly intruded by the dikes of leucogranite (Searle & Fryer, 1986). The Southern Zanskar Mountain Range is located near the Zanskar Shear Zone, which divides the monsoon–dominated HHCS in the south from the somewhat drier and westerly–dominated Tethyan sedimentary sequences in the north (Sharma & Shukla, 2018). The entire valley situated on the northern side of the Great Himalaya, experiences a high altitude semi–desertic condition, because the Southern Zanskar Mountain form a climate barrier, making it difficult for ISM to penetrate this region (Dézes, 1999).

MATERIAL AND METHODS

The lake succession is dominated by sandy–silty sediments. Samples for multi–proxy studies were collected from the ~1.5 m deep excavated sediment profile by pit and channel sampling (Fig. 2). We have sampled the sedimentary profile in a way that each sample represents 2 cm of the profile and a total of 78 samples were collected for the study. We have utilized sediment size/texture (as a proxy for the energy condition and depositional environment), mineral magnetism (proxy for sediment flux or lithogenic input and lithologic variation), carbon isotope signature ($\delta^{13}C_{org}$) preserved in organic constituents of sediments (a proxy for palaeovegetation and climate change), elemental geochemistry (proxy for weathering and erosion) and selected samples for palynofacies data (a proxy for changes in biological organic matter).

Textural analysis

For grain size analysis, 0.5 gm of sediment sample was treated with H_2O_2 to get rid of the organic matter and other soluble salts and subsequently treated with 1N HCl to take out any carbonate fraction. After mixing with a dispersing solution ($(Na_2PO_3)_6$) the samples were disseminated with an ultrasonic oscillator machine for 10 minutes (Yanhong *et al*., 2006). The grain size analyses were done on laser particle size analyzer (LS 13 320) by Beckman Coulter with a size range of 0.004–2000 µm.

Mineral magnetism

The samples were air dried before being packaged in 10 cm^3 non–magnetic plastic vials. Magnetic susceptibility (χ) at a low frequency (0.47 kHz) was measured using a dual sensor on a Bartington Susceptibility Meter (Model MS2). ARM was induced in the samples using a Molspin AF demagnetizer (with an ARM attachment) in a continuous biasing field of 0.1 mT superimposed over a decaying alternating field (a.f.) with a peak field of 100 mT and a decay rate of 0.001 mT per cycle. ARM susceptibility (χARM) was obtained by dividing the mass specific ARM by the biasing field size (0.1 mT = 79.6 A/m). Isothermal Remanent Magnetization (IRM) has been induced in certain samples using an impulse magnetizer (ASC Scientific, USA) at various field strengths (50, 100, 300, 500, 700, and 800 mT) and backfields of up to 300 mT. Remanence was measured using the JR6 (AGICO). In the study, three interparametric ratios were used: frequency–dependent susceptibility (χ fd %), the S–ratio, and the χ_{ARM}/SIRM ratio. The χfd percent figure approximates the average size of ferromagnetic grains. The negative of the ratio of the IRM induced at 300 mT to the SIRM produced at 700 mT

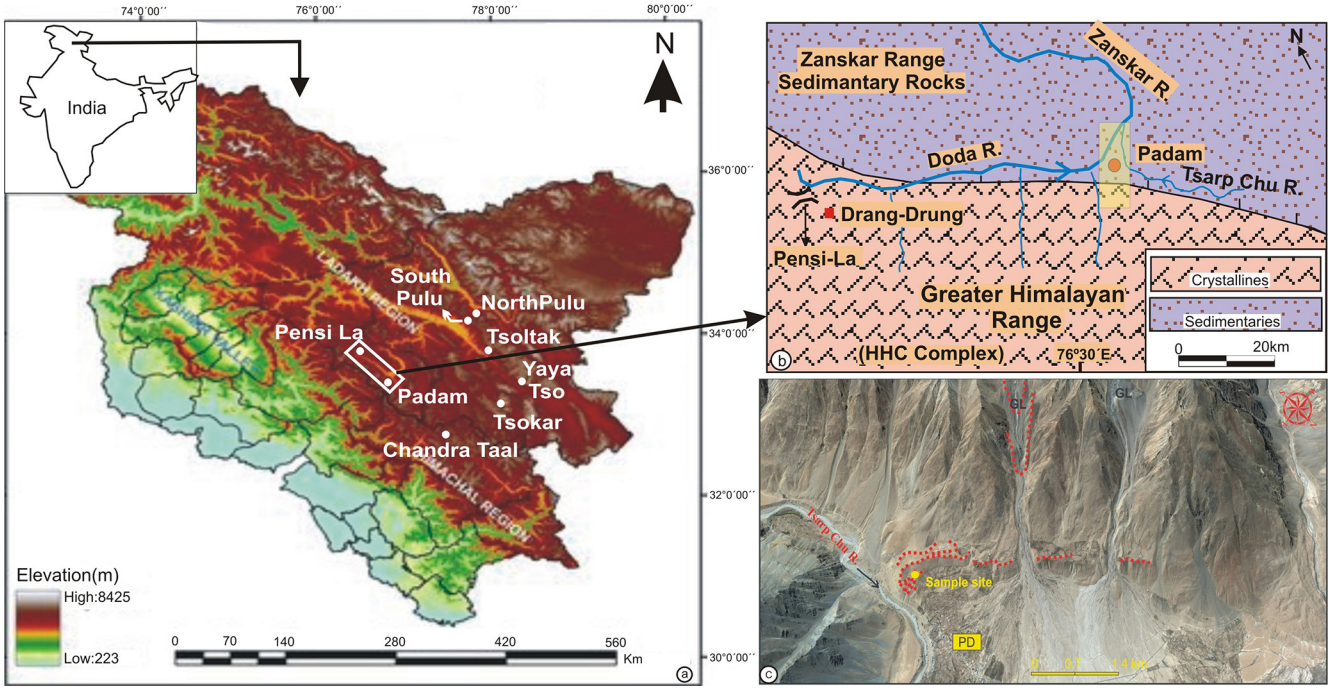

Fig. 1—Map compilation showing (a) Shuttle Radar Topographic Mission (SRTM) Digital Elevation Model (DEM) of western Himalaya showing the present study area (b) Geological map of the Zanskar Valley (after Sharma & Shukla 2018). (c) Google Earth image showing the study area (KP–Khangok–Padam). The yellow circle shows the location of morainal lake (sampling site) and the red dotted lines mark the moraine ridges present on the right flank of Zanskar Valley. GL marks the Glacier Valley that act as a feeder to the study area.

(–IRM–300 mT/SIRM700 mT) is the S–ratio. The grain size is determined by the ARM/SIRM ratio. The IRM acquisition was done on all samples for magnetic mineralogy studies.

Carbon isotope

For carbon isotope analysis ($\delta^{13}C_{org}$), ~1gm of sediment was decarbonised in a hot water bath at 50°C for 2 hours using HCl (5%) and repeated three times. Following that, the samples were centrifuged, washed with deionized water many times until neutral pH was attained, and dried. An auto sampler was used to feed the de–carbonated samples into the Elemental Analyzer (Flash EA 2000 HT). CO_2 gas was created during combustion and injected into a Continuous Flow Isotope Ratio Mass Spectrometer (CFIRMS, MAT 253) linked with a Con–Flow IV interface for isotopic analysis. IAEA CH_3 was used to calibrate the reference gas, and carbon isotopic data was published against Vienna Pee Dee Belemnite (VPDB). International standards (IAEA CH3 and CH_6) and also the internal standards (Sulfanilamide) were used to validate the CO_2 results with an external precision of ±0.1‰ (1σ). The peak area generated from the sum of the integrated m/z 44, 45, and 46 signals detected in the CFIRMS was used to determine total organic carbon (TOC).

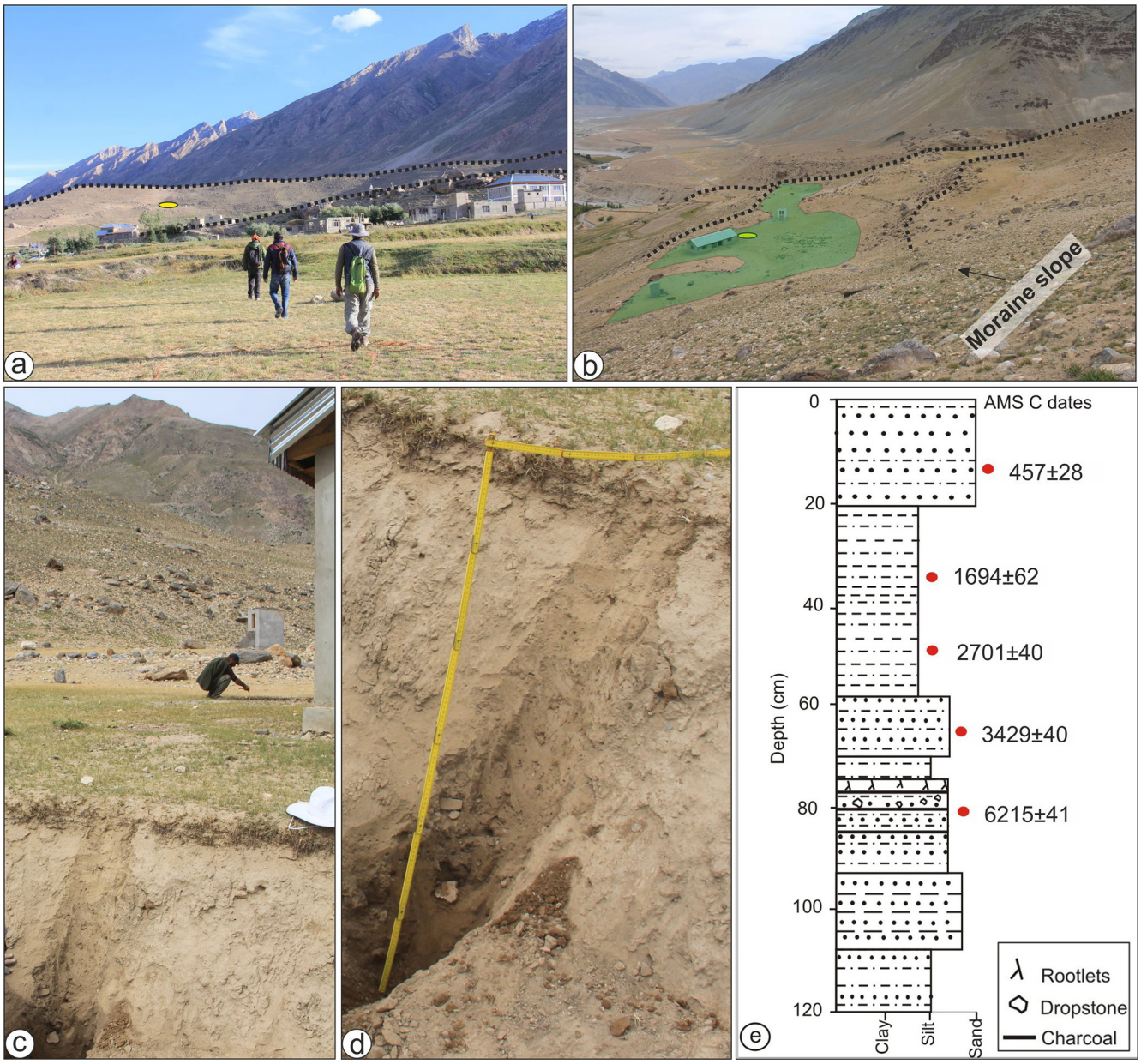

Fig. 2—(a, b) Synoptic view of the study area showing the location of study site (yellow ellipse), (c, d) field photographs showing the study site, (e) Lithology of the Khangok–Padum Sequence.

Elemental analysis

For elemental analysis (Rb and Sr), ~30 mg of each sample was pulverized into fine powder. The digestion of the samples was done in Teflon tubes using a two stage/step digestion process. The materials were digested in Teflon tubes utilising a two–stage/step digestion procedure. The sediment was digested in a 5 ml mixture of hydrofluoric acid and nitric acid, followed by 1 ml per chloric acid ($HClO_4$) and heated to 120°C utilising open digestion (Q–Block operating system) in the first phase. The heating was continued until the acid vapours in the tube stopped evaporating and the sample became entirely dry. The dried residues from the first stage were continued for the second phase by adding 5 ml of HF + HNO_3 (1: 2 ratio), followed by 1 ml of $HClO_4$, and heated to 150° C once more. The tubes were examined for full sediment digestion by adding 2 mL of 5% HNO_3 and monitoring the purity of the solution. If any component remained, the process was repeated until it was completely digested. After that, each tube was rinsed with a 2 percent HNO_3 solution, and the sample was transferred to a volumetric flask to produce a final volume of 50 ml. A comparable digestion method was used for standard reference material (USGS SGR 1B) and blanks. The digested samples, standards, and blanks were evaluated for trace elemental quantities of Rb and Sr using the Agilent Quadrupole 7700 ICP–MS laboratory established at BSIP. The error rate was 10%.

Palynofacies

5 gm sediment was taken for palynofacies analysis of 18 selected samples and processed with 10% HCl and heated in a sand bath for 20 minutes to eliminate the carbonates from the sample. The samples were rinsed three or four times with distilled water before being treated with a 40 percent HF solution to remove the silicates. There was no use of oxidative during maceration. The materials were completely cleaned once more, sieved (20 micron), and the slides were prepped with polyvinyl alcohol and mounted with Canada balsam (Tyson, 1995). The slides were scanned under Olympus BH–2 microscope and photographs captured with a DP–25 camera. The palynofacies recovered were grouped into three broad categories, viz. phytoclast (black oxidized organic matter (OM), partially degraded brown OM, structured OM, degraded brown OM), palynomorphs (viz. pollen/spore, algal/ fungal remains, grass remains, Zoo–remains) and amorphous OM.

INTERPRETATION OF PROXIES USED

The hydro–climatic variations in a region can be inferred from several proxies constituting of physical, chemical and biotic or the combination of the three. The response time of all these proxies to climate forcing can be different temporally due to the lag in proxy response. We have used a combination of the physical, chemical and biotic proxies for a holistic picture of hydro–climate and in turn the palaeoenvironment of the region.

Depending on the transportation medium, particles in nature are often separated by their sizes. Textural analysis gives critical information for determining the energy of the depositional environment. Because the distribution of sizes is related to the availability of different sizes of the parent material and the processes operating, particularly the competency of flow and particle concentrations in suspension, the sand, silt, and clay percentages were calculated in the lake system, with sand deposited in high energy conditions and clay deposited in low energy conditions. TOC concentrations in a lake system can serve as an indirect indication of the kind and biomass of local vegetation (Zhou *et al*., 2004), perhaps reflecting changes in regional hydroclimate. Because the creation, transport, deposition, and modification of magnetic material in a basin reflect climatic conditions and geomorphic processes in the catchment, mineral magnetic characteristics can be used to support evidence of weathering intensity in the source location (Oldfield, 1991). Measuring magnetic susceptibility variations in sediment sections gives insights into weathering, sediment flow, and provenance changes, and can thus contribute useful information for recreating palaeoenvironmental conditions. Several inter–parametric ratios have been worked on. The high value of $\chi_{ARM/}$ SIRM reflects the presence of finer single domain magnetic grain size as χ_{ARM} is sensitive to finer grain size. The S–ratio indicates the ratio of soft IRM and hard IRM, thus discriminative of the presence of magnetite (values close to 1) and haematite in sediments. The stable carbon isotope ($\delta^{13}C_{org}$) values of C_3 plants are mainly controlled by atmospheric CO_2 concentration, mean annual precipitation, light levels, latitude and altitude (Kohn, 2016). There are records which show that mean annual precipitation as well as altitude and latitude are the critical factors regulating the carbon isotopic composition in vegetation (Kohn, 2016; Ali *et al*., 2018). It has been shown that the $\delta^{13}C_{org}$ value of C_3 plants and soil/sediment organic matter under pure C_3 vegetation has a negative correlation with mean annual rainfall amount. The higher Himalayan region is dominated by the C_3 plants, therefore, this region provides a crucial opportunity to ascertain palaeoclimatic variability (Ali *et al*., 2018). The study of palynofacies is critical in the science of palynology for constructing palaeoenvironmental reconstructions and defining depositional habitats in both continental and marine settings (Aggarwal *et al*., 2019). Palynofacies are now acknowledged as a reliable proxy for multi–dimensional investigations such as climatic change, hydrodynamic conditions, oxic–anoxic habitats, runoff related processes, proximal–distal trends, palaeoenvironments, and archaeology research in both continental and marine records. Chemical weathering of surface sediment/rock is mainly governed by the environmental/climatic conditions (Nesbitt

& Young, 1982; Jin *et al*., 2015). The ratio of immobile and mobile elements has been successfully used to measure the degree of weathering (Nesbitt & Young, 1982). Therefore, the temporal variability in the Rubidium to Strontium (Rb/Sr) ratio of the sedimentary sequences has successfully been used as a proxy for degree of weathering (Dasch, 1969; Jin *et. al*., 2006). Strontium (Sr) replaces Ca in the crystal lattice of carbonate minerals and is easily degraded during the weathering process. While, Rubidium (Rb) substitutes for K and shows inert behaviour, and is hard to get weathered hence it is sequestered in the residual phases. Besides this, the bonds between Ca–Sr pair are easy to break during natural processes making them easily mobile resulting in a significant fractionation of Rb and Sr during weathering and deposition. However, there is a contrast in Rb/Sr ratio in loess/palaeosol layers and lacustrine sediments as the former is deposited in an open system, and hence is prone to post depositional leaching. As the lacustrine sediments are deposited in a closed system, the original Rb/Sr ratio is retained. The closed basin lake sediments hence provide an opportunity to understand the climate governed weathering process in changing environments. The Rb/Sr ratio will be high under climatic condition supporting high run–off since both Rb and Sr will enter the lake system due to enhanced weathering. However, with less run–off condition, Sr which is easily weathered will be produced more relative to Rb and therefore the ratio will be low (Jin *et al*., 2006). In this cold, dry location of Zanskar, with no vegetative cover, this proxy reacts in the other manner. During colder periods more material is deposited as a result of physical weathering (as glaciers tend to act as a bulldozing machine and this is a morainal lake), hence the Rb/Sr ratios will be high.

CHRONOLOGY AND AGE–DEPTH MODEL

The Khangok–Padam Lake section is principally composed of silt and sand. The topmost layer is covered by sparse grasses and the top 5 cm show rootlets. Dropstones (cm scale) are encountered at several levels. For establishing the chronology of this sedimentary profile, five bulk samples (organically rich) were dated by accelerator mass spectrometry (AMS^{14}C–radiocarbon dating) at Physical Research Laboratory, Ahmadabad, India. The samples were thoroughly cleaned for any extraneous material. The samples were decarbonated to remove inorganic carbon by using 1M HCl at 80^{o}C. The samples were crushed fine and homogenised. Nearly 1 mg aliquot of organic carbon was taken for its processing with Elemental Analyser, connected to the Automated Graphitization Equipment (M/s IONPLUS, AGE 3). The sample was combusted to produce CO_2, which is transferred to AGE 3 system for conversion to graphite in the presence of iron powder. The graphite powder is pressed into an Al target holder and is loaded for AMS radiocarbon measurement. The radiocarbon measurement of samples was done using HVEE make 1MV AMS (AURiS). The measurements were conducted in several batches along with oxalic acid (OX–II, NBS 465) standard and anthracite as blank along with other reference inter–comparison calibration standards. The radiocarbon ages (uncalibrated) at ~8 cm depth (from top) yielded an age of 384 ± 28 years, at ~34 cm–1773 ± 62, at ~54 cm–2562 ± 40, at ~76 cm–3210 ± 40 and at the bottom ~152 cm an age of 5396 ± 37 years. The radiocarbon ages were calibrated using Intcal13 (Reimer, 2013 and references therein) and considering that the top surface is modern and hence the sample was assumed of 2 ± 1 years and the ages were used to build the age–depth model (Fig. 3). The ages for the profile were interpolated using this age–depth model. The calibration and age–depth model were created in R using the Bchron package (Parnell, 2016; R Core Team, 2014). Total of 78 samples are collected from this sedimentary sequence and on an average each sample represents an average depositional rate of around 2 cm per 106 years. Therefore the study provides a quasi continuous centennial record of climate variability in this area. The sedimentation rate based on actual ages is provided in Fig. 3.

RESULTS

Based on the frequency and variability of the biological, chemical, and physical proxy dataset, four climatic zones (KPZI–KPZIV) have been identified, allowing for the definition of each zone's specific environmental state (Figs 4, 5).

Zone I (KPZ I: ~8200–6200 cal. years BP)

This zone is characterized by two intervals of low sand% and high silt and clay%, gradually increasing χ_{lf}, (varying between 40.8 to 79.1 Values), high and stable χ_{ARM} values, high χARM/SIRM ratio, very low TOC/TN ratio (4–6), variable but higher $\delta^{13}C$ (i.e. < –24‰) and higher Rb/Sr ratio towards the base with decreasing trend towards the top of the zone are noticed. The palynofacies components in this zone (Fig. 5) are dominated by brown degraded organic matter (OM) (10–30%) and oxidized plant tissue (15–32%) with low turnout of black oxidized charcoal and structured OM (10–15%) and absence of fungal remains, spores, animal remains and filamentous algae.

Zone II (KPZ II: ~6200–5280 cal. years BP)

This phase is characterized by relatively fluctuating trend in all the proxy records. The sediments are dominated by ~ 63 % of sand. The χlf values are almost stable except at 77–77.5 cm depth (~5788–5740 cal. years BP) but highly fluctuating; S–ratio record an abrupt rise from preceding zone which further increases at ~5740 cal years BP; low χARM; stable but fluctuating χARM/SIRM; low Rb/Sr ratio; sharp increase in TOC/TN ratio and lower $\delta^{13}C$ values are recorded especially

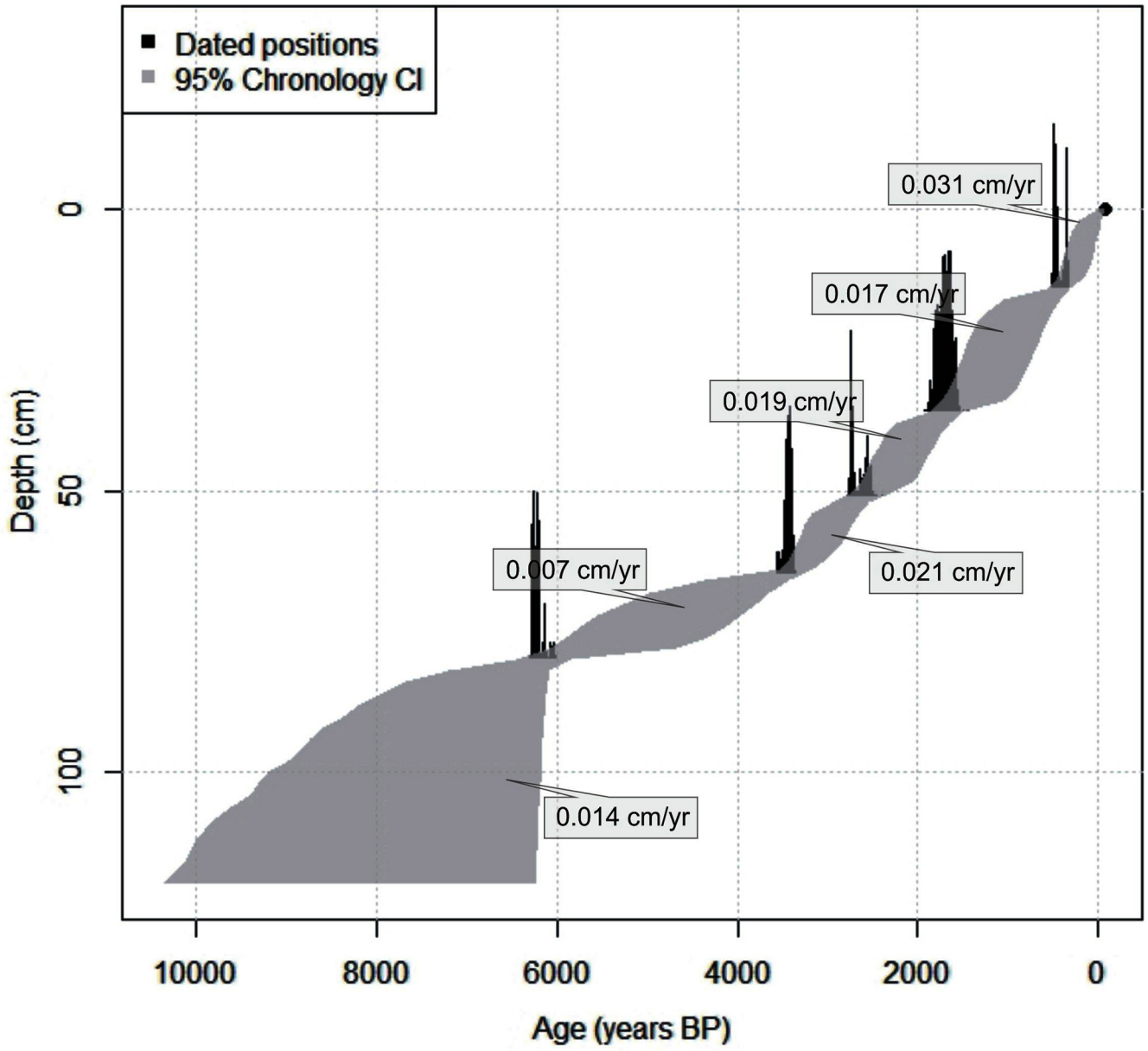

Fig. 3—Basin age depth chronology for the sediment section.

again at ~5788–5740 cal. years BP pointing towards an abrupt short–lived climatic event around this period. Black oxidised OM shows an increase along with the structured brown OM, fungal remains, spores and filamentous algae show presence in this zone.

Zone III (KPZ III: ~5280–457 cal. years BP)

In this zone, clay and silt show a gradually decreasing trend; χlf values also manifest a progressive decrease along with stable s–ratio, high χARM/SIRM ratios; gradually decreasing χARM, relatively higher and stable Rb/Sr till ~3400 cal. Years BP and then showing comparatively lower values; till ~457 cal. years BP to the top of this zone. This zone is also marked by relatively higher $\delta^{13}C$ values that show a lowering trend towards the top. TOC/TN fluctuates between 7 and 12 and shows a rising trend till ~3200 cal. years BP and then decreases till the top of this zone. The black oxidized OM decreases as seen at both levels (~2300 and ~900 cal. years BP), pollen/spores, fungal remains, grass remains oxidized tissue and filamentous algae also persists in varying capacities.

Zone IV (KPZ IV: ~457–present cal. years BP)

This zone is dominated by sand and silty fraction. During the last 500 years a subtle change (lowering) in the proxy

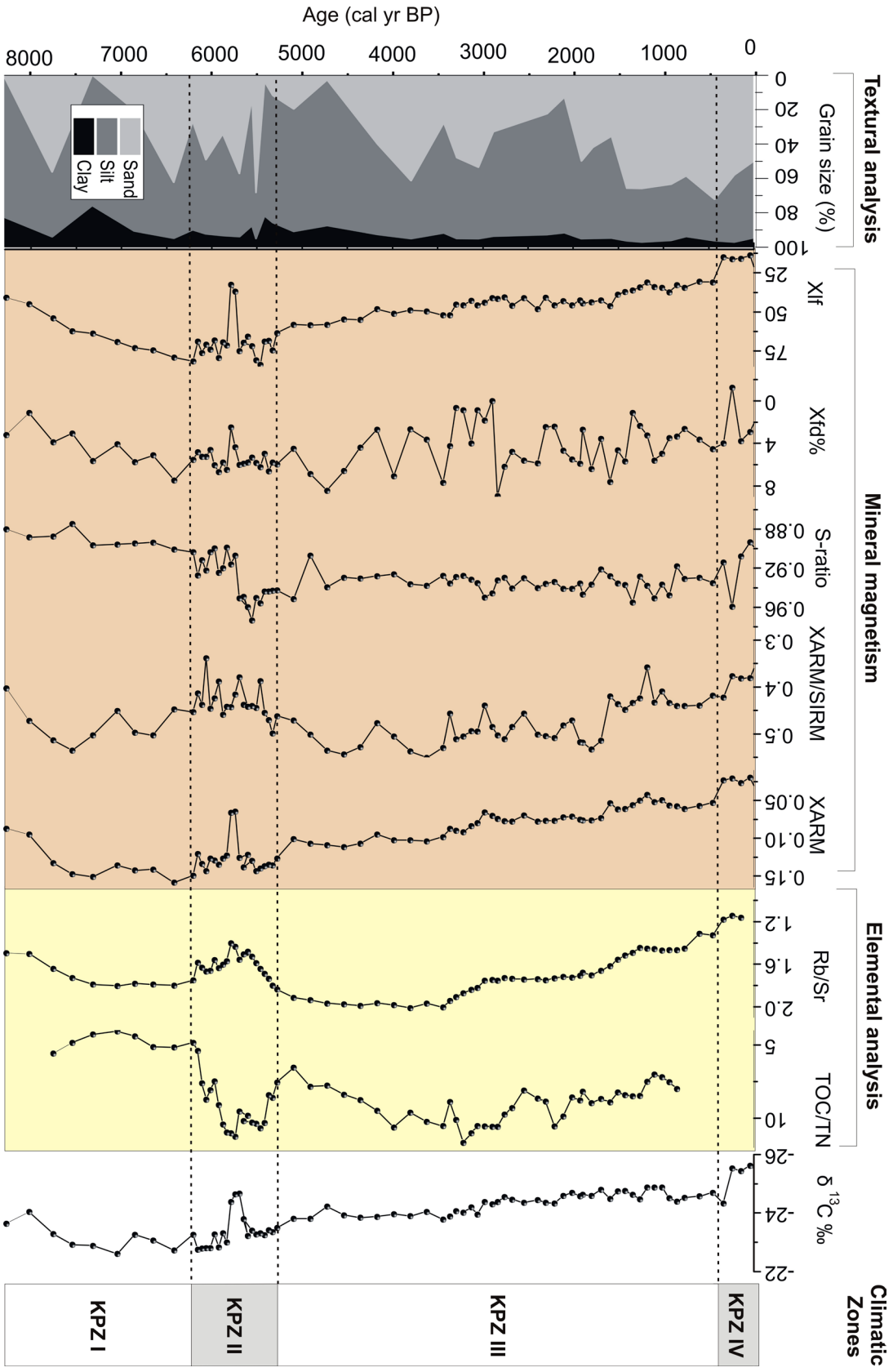

Fig. 4—Temporal variability and correlation in grain size (Sand, silt and clay %), mineral magnetic parameters (χlf,fd%, S–ratio, χARM/SIRM, χARM)), elemental analysis (Rb/Sr and TOC/N ratio) and measured $\delta^{13}C$ value (‰; VPDB).

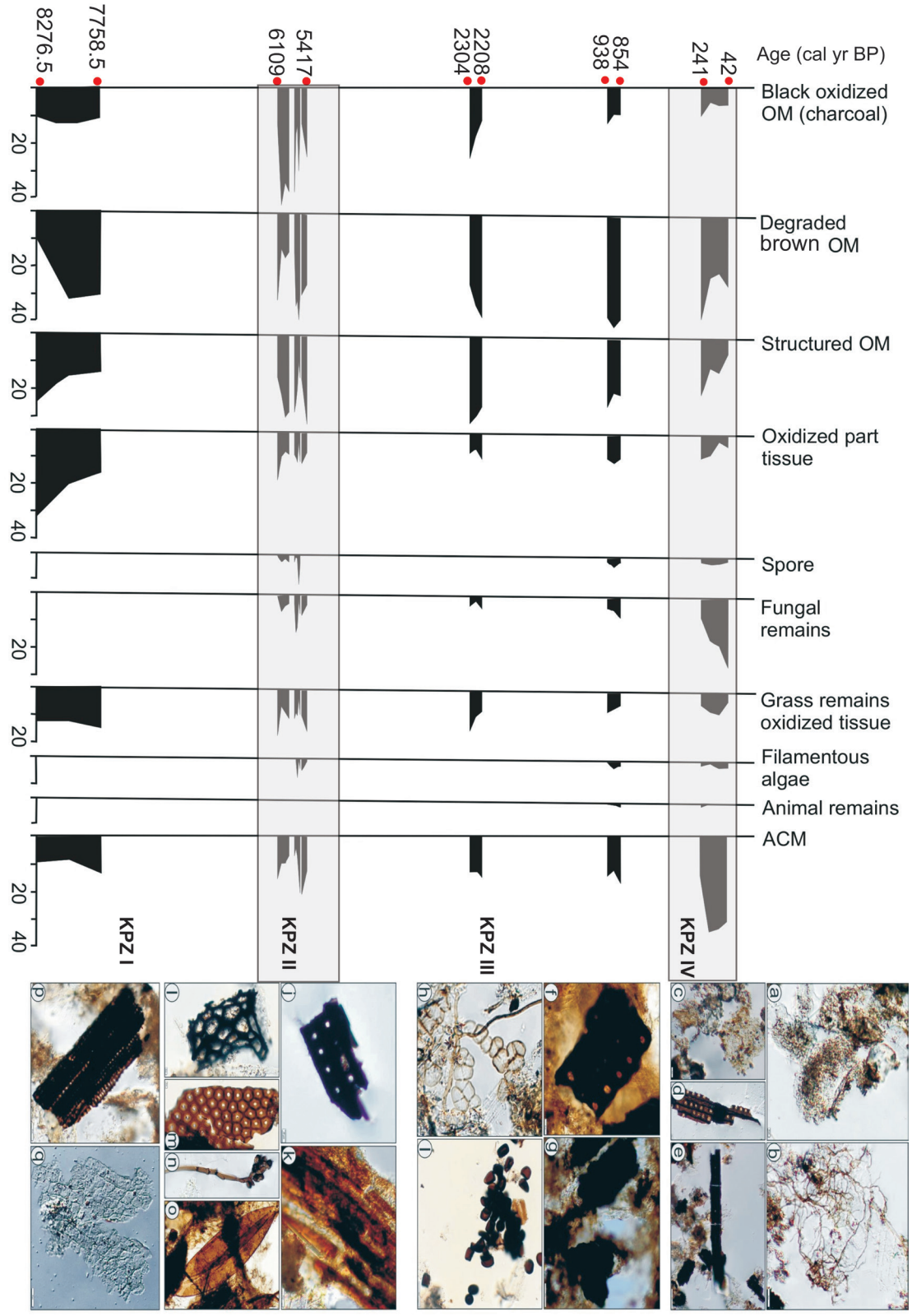

Fig. 5—Palynofacies distribution in the different climatic zones of the Khangok–Padum section; Photographs of the recovered palynofacies–(a) Amorphous organic matter (OM); (b) Fungal Mycelium; (c) Degraded brown OM; (d) Structured OM; (e) Black oxidized OM; (f) Degraded brown OM; (g) Black oxidized OM; (h, i) Fungal remains (spores); (j) Black oxidized OM; (k) Degraded brown OM; (l, m) Structured OM; (n) Fungal Mycelium; (o) Poaceae pollen; (p, s) Black oxidized OM; (q) Oxidized plant tissue; (r) Structured OM.

values is observed. The overall trend of the proxies during this phase like the $\delta^{13}C$ values, magnetic susceptibility as well as the Rb/Sr ratio show further lower values. The palynofacies component is dominated by Amorphous OM (31–35%), brown degraded OM (20–25%) and fungal remains (15–25%) with low turnout of Structured OM (5–12%) and black oxidized charcoal (3–4%). The fungal remains comprising of *Glomus* sp. clearly show evidences of local erosion from the lake vicinity.

DISCUSSION

The entire Zanskar Basin has witnessed multiple glacier advances in the past (Taylor & Mitchell, 2000; Hedrick *et al*., 2011) which is clearly manifested by its typical glacial geomorphology (Sharma & Shukla, 2018). The presence of huge lateral moraines near the Padum Village suggests extensive glacier cover in this valley. These lateral moraines have been found to shelter morainal lake sediments that have been used in the present study to understand the past hydroclimatic conditions in this area. Moraine lakes occupy a depression that results from irregular deposition of drift in the ridges of an end or lateral moraine suite of a glacier, and are dominantly recharged by the meltwater (Song *et al*., 2017). These lakes thus can be intrinsically linked to climate. The present study documents multi–proxy record of palaeoclimate and hydroclimatic variability reconstructed using relict morainal lake sediments from this (Zanskar) climatologically sensitive transitional zone since the last ~8200 cal years BP. Glaciers and lakes are often regarded as useful and sensitive markers of past climate change, and hence the Khangok–Padam Lake is critical to understanding climatic variability in the Zanskar region. The Khangok–Padam Lake sampled for the present study, is fed by the insolation driven meltwater/runoff that regulated the temporal changes in the sediment influx and recorded the variations in other proxies. Between ~8200–6200 cal years BP the gradually increasing χlf, low TOC/TN and higher $\delta^{13}C$ values along with better phytoclasts dominated by degraded brown OM and structured OM suggest that the area witnessed a mild precipitation/runoff condition; gradually increasing towards the top. The χlf and Rb/Sr values suggest an enhanced flux of terrestrial organic matter from the catchment area towards the top of the zone. During the period the palynofacies association are dominated by brown degraded OM and oxidized plant tissue with low black oxidized charcoal and structured OM proportions. The present deposition indicates that the phytoclasts were the major components in the depositional phase and were transported due to higher fluvial activity and very low accommodation space. The overall climatic scenario is of improving conditions from 8000–6200 cal. years BP. In the west of the study area, decline of the lake levels has been reported at ~6800 cal. years BP and an arid phase has been suggested in the region between 6800–5200 cal. years BP. Although the bigger lakes did exist during this time, the lake level got lowered. This declining trend in hydroclimatic conditions has been attributed to the ISM and has resulted in increasing aridity in the Ladakh and the adjacent Trans–Himalaya ranges since ~6000 cal. years BP (Prasad & Enzel, 2006). Being in a climatologically transitional zone, the moisture availability and fluctuating proxy records do point at the role of both ISM and Westerly forcing to control the hydroclimatic variability of this particular region. Based on the variations in the present proxy data, it is suggested that the KPZ I has experienced a mild cold (from cool and dry to moderate cool and dry climatic conditions) climatic phase. Our interpretation is strengthened by recent glacial–chronological data, which show that a cool/dry phase occurred after 6.3 and before 5.1 ka in the Zanskar Valley and has been attributed to an overall weakened ISM (Wünnemann *et al*., 2010; Bhushan *et al*., 2018; Sharma & Shukla, 2018). This implies that during this time, the glaciers also responded to a weakened insolation driven monsoon at the expense of enhanced westerlies (Wünnemann *et al*., 2010; Bhushan *et al*., 2018; Ali *et al*., 2020). The weakening of the ISM during ~5800 to 5000 cal years BP has also been reported by Bhushan *et al*. (2018) from the ISM dominated Central Himalaya. The palynofacies in this period suggests that the transport of water was continuous but stagnant conditions also prevailed giving conductively environment for the commencement of lake formation that may have been resulted due to weakening of ISM in and around this region.

This cool/dry phase is subsequently followed by prominent changes in all the proxies during KPZ II: ~6200–5280 cal. years BP. The overall trends of the proxies manifest climatic amelioration and hence improved hydroclimatic conditions in this region. In Tsoltak record a wet phase with stable and high lake levels has been reported between 6400–5170 cal. years BP (Joshi *et al*., 2021). Our inferences are in agreement with the recent study from Ladakh Range (Tsoltak record) as well as from Chandra Valley where an increasing trend of all the arboreal pollen elements suggests warm and moist condition (Rawat *et al*., 2015). This is further substantiated by lower $\delta^{13}C$ values advocating for warm and high precipitation condition during the mid Holocene in the Chandra Valley, which experiences similar climatic conditions as Zanskar Valley. Our $\delta^{13}C$ data also reveal a significant decrease, indicating improved hydroclimatic conditions in this region during the active ISM phase, which coincides to the Holocene Climatic Optima (HCO) Era (Rawat *et al*., 2015). Hence the present study and the earlier records of HCO from different Himalayan regions like Kashmir, TsoKar Lake (Ladakh), Mari (Himachal Pradesh), Surinsar (Jammu), Dhakuri Peat (Uttarakhand) and Chandra Peat (Himachal Pradesh) (Bhattacharyya, 1988; Phadtare, 2000; Demske *et al*., 2009; Rawat *et al*., 2015) suggest a regional response to the climatic drivers during the mid–Holocene. Similarly, based on multiproxy data, Bali *et al.* (2017) and Srivastava *et al*. (2018) suggested a warm and wetter/humid climate in

the ISM dominated Kedarnath Valley, central Himalaya and Triloknath Valley, western Himalaya.

Following this relatively enhanced hydroclimatic phase, between ~5280–457 cal. years BP initiation of a stable climate with moderate hydroclimatic conditions in Khanjok–Padam region are observed. During this zone/phase, a progressive lowering of $\delta^{13}C$ values, relatively higher Rb/Sr and TOC/TN ratio and decreasing magnetic susceptibility is observed. Based on the proxy data a progressive improvement in the overall climatic conditions is inferred. It is intriguing to note that even the 4.2 ka cold event and the 2.6 ka arid event recorded well from the Ladakh region, do not show any prominent changes here. The change is an overall gradual one, with a more or less stable moisture source. Our data is in conformity with the other palaeoclimatic records from the central Himalaya, where in a moderate to weak hydroclimatic conditions have been reported by Bhushan *et al*. (2018). Similarly, Bali *et al*. (2017) have also reported a lesser ISM during ~5300–2200 cal years BP from the Triloknath Valley. Based on $\delta^{13}C$, TOC and pollen data, Rawat *et al*. (2015) have also inferred moderate ISM (punctuated by a wet spell) during the late Holocene in the climatologically similar Chandra Valley. The gradually improving hydroclimatic conditions during the later part of the Holocene have also been reported in a number of studies from the adjoining valleys in Ladakh (Ali *et al*., 2020; Joshi *et al*., 2021; Phartiyal *et al*., 2020; 2021a; Fig. 6). This phase indicates lowering of runoff and very high degradation of palynofacies due to high Amorphous OM. The fungal remains comprising of *Glomus* sp. clearly evidences local erosion from the lake vicinity.

The youngest KPZ IV (~500–present cal. years BP) is characterized by further lowering of $\delta^{13}C$ values, magnetic susceptibility and Rb/Sr ratio (Fig. 4). The sand percentage is higher, and the silt content also show increasing trend, implying enhanced hydroclimatic conditions. Improving hydroclimatic conditions in the Ladakh region have been reported in a number of studies (Ali *et al*., 2020; Joshi *et al*., 2021; Phartiyal *et al*., 2020; 2021a). Besides the Ladakh Himalaya, records of improving hydroclimatic conditions during the last ~500 cal. years BP have also been reported from a number of locations in the ISM governed central Himalayan sector (Bhushan *et al*., 2018 and references therein). Although, the signatures of LIA are not prominent in the relict lake sequence, however in the Northern Hemisphere, the LIA glacial advance happened between 1400 and 1900 CE, however the glacier advances related to the global LIA occurred between 1300 and 1600 CE, slightly earlier than the coldest period of Northern Hemisphere (Rowan, 2017). This early cooling has been related to a southerly shift in the Asian monsoon, more Westerly winter precipitation, and wetter conditions in the Himalaya (Rowan, 2017). Following the LIA cooling, a prominent decrease in $\delta^{13}C$ values and Rb/Sr ratio indicate climate amelioration. Palynofacies data suggest that the lake captured by high sediment content and the water level would have been lower as compared to previous stages. The palynofacies data also shows dominance of amorphous OM followed by degraded brown OM, fungal remains and structured OM. The data indicates that the lake shallowed during this period followed by high degradation of OM (Fig. 5). We propose that the lake got filled with sediments and spill over started. Regional (high Asia) climatic proxy data also demonstrate 20th Century warming in context of the past millennium (Shekhar *et al*., 2017). This means that rising temperatures increased snow and glacier melt, as well as the atmosphere's moisture–holding capacity, all of which have a direct impact on precipitation patterns and severity (Trenberth *et al*., 2003).

Figure 6 shows a comparison of the studied records from the Tethyan Himalaya (Khangok–Padam; PensiLa, Tsokar, Chandra Peat bog) and Trans Himalaya (Spituk, North and South Pulu, Tsoltak and YayaTso) and Tibetan Plateau region (Guliya) to get the overall picture of the change of the climatic and moisture pattern. The progressive improvement in the hydrological conditions during the last ~6.3 cal. years BP from Khangok–Padam, Zanskar Valley as inferred from the multiproxy data show a synchrony with other regional studies from the Indian subcontinent (Fig. 6; Kotlia *et al*., 2015; Bali *et al*., 2017; Phadtare, 2000; Phartiyal *et al*., 2020; 2021a, b). Orbitally modulated change in solar radiation can cause large temperature gradient in the northern continent that results in shift of the Inter Tropical Convergence Zone (ITCZ) and the subtropical jet. Increased solar radiation can cause warming of the Northern Hemisphere and lead to a northward shift of ITCZ and jet stream resulting in increased precipitation to NW Himalaya, Tibetan region and north–northeast China. Hydroclimatic changes in the study area may be attributed to the mid–Northgrippian (mid–Holocene) solar irradiance, which has been suggested to be a relatively higher (Crowley & North, 1991; Rupper *et al*., 2009). Despite a regional spatio–temporal heterogeneity in the climate reconstructions during the mid to late Northgrippian from the study area, overall a lower amplitude, complex array of natural forcings, feedbacks, and internal variability operating in the climate system has been implicated.

CONCLUSION

Four prominent hydroclimatic phases mark the Holocene epoch in Khangok–Padam, Zanskar (~8200–6200; ~6200–5400; ~5400–460 and ~500 to present). Centennial–scale palaeoenvironmental variability has been described using multi–proxy analysis (textural analysis, environmental magnetic parameters, stable carbon isotopes, palynofacies and elemental concentration). The first trend is punctuated by an abrupt wet spells at ~6200–5200 cal years BP (mid Holocene) and show signatures of relatively drier climate during the LIA. The main driving forces implicated for the changes seen to be the solar output variations. However, the area lying in a

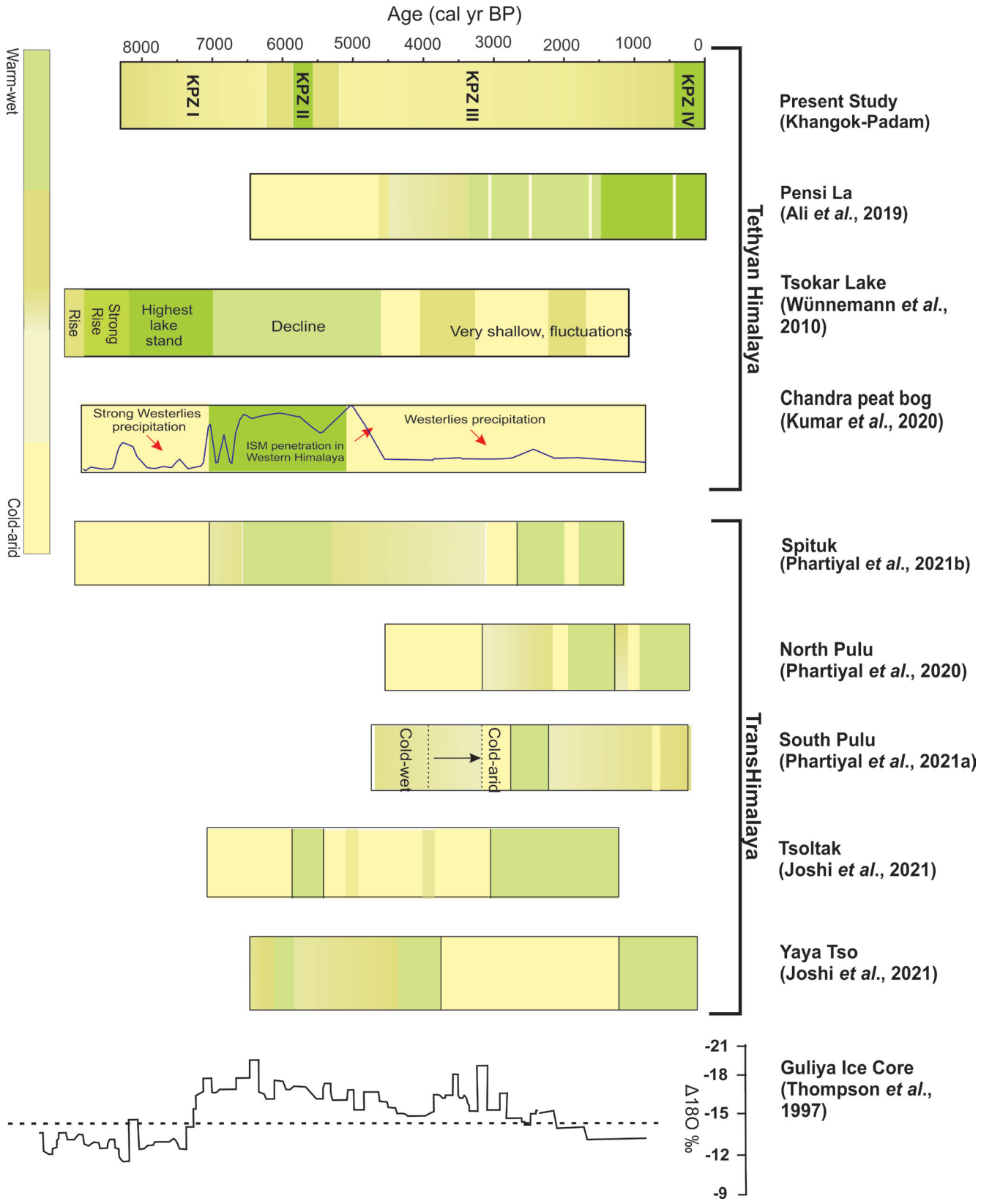

Fig. 6—Comparison and review of the studied hydroclimate and palaeoclimatic records from the Tethyan Himalaya (Khangok–Padam; PensiLa, Tsokar, Chandra Peat bog) and Trans Himalaya (Spituk, North and South Pulu, Tsoltak and YayaTso) and Tibetan Plateau region (Guliya) for a regional picture.

transitional zone of NW Himalaya shows no emphatic record of the events like the 4.2 ka, 2.6 ka and Holocene Climatic Optima. Contrary to the earlier studies in the north western Himalaya (e.g. Tsokar and TsoMorari), our results show an increasing hydroclimatic condition in this transition zone between the Higher and Trans Himalaya.

Acknowledgements*—This work was performed under the auspices of Birbal Sahni Institute of Palaeosciences, Lucknow, India (BSIP/RDCC/5/2022–23). SAIF–BSIP is acknowledged for the infrastructural facilities. Special thanks are to the Ladakh Administrative Authorities and Wild Life Department for providing necessary permissions during the field work. Reviewers are thanked for their valuable suggestions.*

REFERENCES

Aggarwal N, Agrawal S & Thakur B 2019. Palynofloral, palynofacies and carbon isotope of Permian coal deposits from the Godavari Valley Coalfield, South India: Insights into the age, palaeovegetation and palaeoclimate. International Journal of Coal Geology 214: 103285

Ali SN, Dubey J, Ghosh R, Quamar MF, Sharma A, Morthekai P, Dimri AP, Shekhar M, Arif Md & Agarwal S 2018. High frequency abrupt shifts in the Indian summer monsoon since Younger Dryas in the Himalaya. Scientific reports 8: 9287.

Ali SN, Agrawal S, Sharma A, Phartiyal B, Morthekai P, Govil P, Bhushan R, Farooqui S, Jena PS & Shivam A 2019. Holocene hydroclimatic variability in the Zanskar Valley, Northwestern Himalaya, India. Quaternary Research 1–17, 10.1017/qua.2020.22.

Ali SN, Morthekai P, Bajpai S, Phartiyal B, Sharma A, Quamar MF & Prizomwala S 2020. Redefining the timing of Tongul glacial stage in the Suru Valley, NW Himalaya, India: New insights from luminescence dating. Journal of Earth System Science 129 (16): 1–11.

Bali R, Chauhan MS, Mishra AK, Ali SN, Tomar A, Khan I, Singh DS & Srivastava P 2017. Vegetation and climate change in the temperate–subalpine belt of Himachal Pradesh since 6300 cal. years. B.P., inferred from pollen evidence of Triloknath palaeolake. Quaternary International 444: 11–23.

Banerji US, Arulbalaji P & Padmalal D 2020. Holocene climate variability and Indian Summer Monsoon: An overview. Holocene 30: 744–773.

Bhattacharyya A 1988. Vegetation and climate during postglacial in the vicinity of Rohtang Pass, Great Himalayan Range. Pollen & Spores 30: 417–427.

Bhushan R, Sati SP, Rana N, Shukla AD, Mazumdar AS & Juyal N 2018. High–resolution millennial and centennial scale Holocene monsoon variability in the Higher Central Himalayas. Palaeogeography Palaeoclimatology Palaeoecology 489: 95–104.

Bolch T, Kulkarni A, Kääb A, Huggel C, Paul F, Cogley JG, Frey H, Kargel JS, Fujita K, Scheel M & Stoffel M 2012. The state and fate of Himalayan glaciers. Science 336: 310–314.

Crowley TJ & North GR 1991. Paleoclimatology. New York: Oxford University Press.

Dasch EJ 1969. Strontium isotopes in weathering profiles, deep–sea sediments, and sedimentary rocks. Geochimica & Cosmochimica Acta 33: 1521–1552.

Demske D, Tarasov PE, Wünnemann B & Riedel F 2009. Late glacial and Holocene vegetation, Indian monsoon and westerly circulation dynamics in the Trans–Himalaya recorded in the pollen profile from high altitude TsoKar Lake, Ladakh, NW India. Palaeogeography Palaeoclimatology Palaeoecology 279: 172–185.

Dézes P 1999. Tectonic and metamorphic evolution of the central Himalayan domain in southeast Zanskar (Kashmir, India) [thesis]. Universit´e de Lausanne.

Hedrick KA, Seong YB, Owen LA, Caffee MW & Dietsch C 2011. Towards defining the transition in style and timing of Quaternary glaciation between the monsoon–influenced Greater Himalaya and the semi–arid Transhimalaya of Northern India. Quaternary International 236: 21–33.

Jin Z, An Z, Yu J, Li F & Zhang F 2015. Lake Qinghai sediment geochemistry linked to hydroclimate variability since the last glacial. Quaternary Science Reviews 122: 63–73.

Jin Z, Cao J, Wu J & Wang S 2006. A Rb/Sr record of catchment weathering response to Holocene climate change in Inner Mongolia. Earth Surface Processes and Landforms. The Journal of the British Geomorphological Research Group 31: 285–291.

Joshi P, Phartiyal B & Joshi M 2021. Hydro–climatic variability during last five thousand years and its impact on human colonization and cultural transition in Ladakh sector, India. Quaternary International 599–600: 45–54.

Kathayat G, Cheng H, Sinha A, Yi L, Li X, Zhang H, Li H, Ning Y & Edwards RL 2017. The Indian monsoon variability and civilization changes in the Indian subcontinent. Science Advances 3: e1701296, 1126/sciadv.1701296.

Kohn MJ 2016. Carbon isotope discrimination in C3 land plants is independent of natural variations in pCO2. Geochemical Perspectives Letters 2: 35–43, 10.7185/geochemlet.1604.

Kotlia BS, Singh AK, Joshi LM & Dhaila BS 2015. Precipitation variability in the Indian Central Himalaya during last ca. 4000 years inferred from a speleothem record: impact of Indian Summer Monsoon (ISM) and Westerlies. Quaternary International 371: 244–253.

Kumar O, Ramanathan AL, Bakke J, Kotlia BS & Shrivastava JP 2020. Disentangling source of moisture driving glacier dynamics and identification of 8.2 ka event: evidence from pore water isotopes, Western Himalaya. Scientific Reports, 15324, 10.1038/s41598–020–71686–4.

Leipe C, Demske D & Tarasov P 2014. A Holocene pollen record from the northwestern Himalayan lake TsoMoriri: implications for palaeoclimatic and archaeological research. Quaternary International 348: 93–112, 10.1016/j.quaint.2013.05.005.

Mishra PK, Prasad S & Anoop A 2015. Carbonate isotopes from high altitude TsoMoriri Lake (NW Himalayas) provide clues to late glacial and Holocene moisture source and atmospheric circulation changes. Palaeogeography Palaeoclimatology Palaeoecology 425: 76–83, 10.1016/j.palaeo.2015.02.031.

Nesbitt HW & Young GM 1982. Early Proterozoic climates and plate motions inferred from element chemistry of lutites. Nature 299: 715–717, 10.1038/299715a0.

Oldfield F 1991. Environmental Magnetism: A personal perspective. Quaternary Science Reviews 10: 73–85, 10.1016/0277–3791(91)90031–O.

Parnell A 2016. Bchron: Radiocarbon dating, age–depth modelling, relative sea level rate estimation, and non–parametric phase modelling. R package version 4.1.1. http: //CRAN.R–project.org/package=Bchron.

Petit JR, Jouzel J, Raynaud D, Barkov NI, Barnola JM, Basile I, Bender M, Chappellaz J, Davis M, Delaygue G, Delmotte M, Kotlyakov VM, Legrand M, Lipenkov VY, Lorius C, Pepin L, Ritz C, Saltzman E & Stievenard M 1999. Climate and atmospheric history of the past 420,000 years from the Vostok ice core, Antarctica. Nature 399: 429–436, 10.1038/20859.

Phadtare NR 2000. Sharp decrease in summer monsoon strength 4000–3500 cal. years B.P. in the higher Himalaya of India based on pollen evidence from alpine peat. Quaternary Research 53: 122–129, 10.1006/qres.1999.2108.

Phartiyal B, Randheer S, Priyanka J & Nag D 2020. Late–Holocene climatic record from a glacial lake in Ladakh range, Trans–Himalaya, India. Holocene 30: 1029–1042, 10.1177/0959683620908660.

Phartiyal B, Singh R, Nag D, Sharma A, Agnihotri R, Prasad V, Yao T, Yao P, Joshi P, Balasubramanian K, Singh SK & Thakur B 2021a. Reconstructing climate variability during the last four millennia from Trans–Himalaya (Ladakh–Karakoram, India) using multiple proxies. Palaeogeography Palaeoclimatology Palaeoecology 562: 110142, 10.1016/j.palaeo.2020.110142

Phartiyal B, Nag D & Joshi P 2021b. Holocene climatic record of Ladakh,

Trans–Himalaya. *In*: Kumaran N & Padmalal D (Editors)–Holocene climate change and environment. Elsevier: 61–88

Prasad S, Anoop A, Riedel N, Sarkar S, Menzel P, Basavaiah N, Krishnan R, Fuller D, Plessen B, Gaye B, Röhl U, Wilkes H, Sachse D, Sawant R, Wiesner M & Stebich M 2014. Prolonged monsoon droughts and links to Indo–Pacific warm pool: a Holocene record from Lonar Lake, central India. Earth Planetary Science letters 391: 171–182, 10.1016/j.epsl.2014.01.043.

Prasad S & Enzel Y 2006. Holocene palaeoclimates of India. Quaternary Research 66: 442–453, 10.1016/j.yqres.2006.05.008.

Pratt–Sitaula B, Burbank DW, Heimsath AM, Humphrey NF, Oskin M & Putkonen J 2011. Topographic control of asynchronous glacial advances: A case study from Annapurna, Nepal. Geophysical Science Letters 38: L24502, 10.1029/2011GL049940

R Core Team 2014. R: A Language and Environment for Statistical Computing. R Foundation for Statistical Computing, Vienna, Austria. URL https: //www.R–project.org/.

Rawat S, Gupta AK, Sangode SJ, Srivastava P & Nainwal HC 2015. Late Pleistocene–Holocene vegetation and Indian summer monsoon record from the Lahaul, Northwest Himalaya, India. Quaternary Science Reviews 114: 167–181, 10.1016/j.quascirev.2015.01.032.

Reimer PJ 2013. Intcal13 and Marine13 Radiocarbon age calibration curves 0–50,000 Years Cal BP. Radiocarbon 55: 1869–1887.

Rowan AV 2017. The 'Little Ice Age' in the Himalaya: A review of glacier advance driven by Northern Hemisphere temperature change. Holocene 27: 292–308, 10.1177/0959683616658530.

Rupper S, Roe G & Gillespie A 2009. Spatial patterns of Holocene glacier advance and retreat in Central Asia. Quaternary Research 72: 337–346,10.1016/j.yqres.2009.03.007.

Sarkar S, Prasad S, Wilkes H, Riedel N, Stebich M, Basavaiah N & Sachse D 2015. Monsoon source shifts during the drying mid–Holocene: Biomarker isotope based evidence from the core 'monsoon zone' (CMZ) of India. Quaternary Science Reviews 123: 144–157, 10.1016/j.quascirev.2015.06.020.

Searle MP & Fryer BJ 1986. Garnet, tourmaline and muscovite–bearing leucogranites, gneisses and migmatites of the Higher Himalayas from Zanskar, Kulu, Lahoul and Kashmir. Geological Society, London, Special Publications 19: 85–201.

Sharma A & Phartiyal B 2018. Late Quaternary palaeoclimate and contemporary moisture source to extreme NW India: A review on present understanding and future perspectives. Frontiers of Earth Science 6, 10.3389/feart.2018.00150.

Sharma S & Shukla AD 2018. Factors governing the pattern of glacier advances since the Last Glacial Maxima in the transitional climate zone of the Southern Zanskar Ranges, NW Himalaya. Quaternary Science Reviews 201: 223–240, 10.1016/j.quascirev.2018.10.006

Shekhar M, Bhardwaj A, Singh S, Ranhotra PS, Bhattacharyya A, Pal AK, Roy I, Martín–Torres FJ & Zorzano M 2017. Himalayan glaciers experienced significant mass loss during later phases of little ice age. Scientific Reports7: 10305, 10.1038/s41598–017–09212–2

Song C, Sheng Y, Wang J, Ke L, Madson A & Nie Y 2017. Heterogeneous glacial lake changes and links of lake expansions to the rapid thinning of adjacent glacier termini in the Himalayas. Geomorphology 280: 30–38, 10.1016/j.geomorph.2016.12.002.

Srivastava P, Agnihotri R, Sharma D, Meena NK, Sundriyal YP, Saxena A, Bhushan R, Sawlani, R, Banerji U, Sharma C, Bisht P, Rana N & Jayangondaperumal R 2018. 8000–year monsoonal record from Himalaya revealing reinforcement of tropical and global climate systems since mid–Holocene. Scientific Reports 7**:** 14515, 10.1038/s41598–017–15143–9.

Sun J, Zhou T, Liu M, Chen Y, Shang H, Zhu L, Shedayi AA, Yu H, Cheng G, Liu G, Xu M, Deng W, Fan J, Lu X & Sha Y 2018. Linkages of the dynamics of glaciers and lakes with the climate elements over the Tibetan Plateau. Earth Science Reviews 185: 308–324, 10.1016/j.earscirev.2018.06.012.

Taylor PJ & Mitchell WA 2000. The Quaternary glacial history of the Zanskar Range, north–west Indian Himalaya. Quaternary International 65: 81–99.

Thompson LG, Yao T, Davis ME, Henderson KA, Mosley–Thompson E, Lin PN, Beer J, Synal HA, Cole–Dai J & Bolzan JF 1997. Tropical climate instability: the last glacial cycle from a Qinghai–Tibetan ice core. Science 276: 1821–1825.

Trenberth KE, Dai A, Rasmussen RM & Parsons DB 2003. The changing character of precipitation. Bulletin American Meteorological Society 84: 1205–1217.

Tyson RV 1995. Sedimentary Organic Matter. Organic facies and palynofacies. Chapman and Hall: London.

Wünnemann B, Demske D, Tarasov P, Kotlia B, Reinhardt–Imjela C, Bloemendal J, Diekmann B, Hartmann K, Krois J, Riedel F & Arya N 2010. Hydrological evolution during the last 15k years in the TsoKar Lake Basin (Ladakh, India), derived from geomorphological, sedimentological and palynological records. Quaternary Science Reviews 29: 1138–1155.

Yanhong W, Lücke A., Zhangdong J, Sumin W, Schleser GH, Battarbee RW & Weilan X 2006. Holocene climate development on the central Tibetan Plateau: a sedimentary record from Cuoe Lake. Palaeogeography Palaeoclimatology Palaeoecology 234: 328–340.

Zhou W, Yu X, Jull AJ, Burr G, Xiao JY, Lu X & Xian F 2004. High–resolution evidence from southern China of an early Holocene optimum and a mid–Holocene dry event during the past 18,000 years. Quaternary Research 62: 39–48.